Supplementary Materials for

Observed winter Barents Kara Sea ice variations induce prominent sub-decadal variability and a multi-decadal trend in the Warm Arctic Cold Eurasia pattern

Rohit Ghosh*[1,2,3], Elisa Manzini[1], Yongqi Gao[4] †, Guillaume Gastineau[5], Annalisa Cherchi[6,7], Claude Frankignoul[5,8], Yu-Chiao Liang[9,8], Young-Oh Kwon[8], Lingling Suo[4], Evangelos Tyrlis[10], Jennifer V. Mecking[11,12], Tian Tian[13], Ying Zhang[14], Daniela Matei[1]

*Corresponding author. Email: rohit.ghosh@awi.de

[1] Max-Planck-Institute for Meteorology, Hamburg, Germany

[2] Department of Meteorology, University of Reading, Reading, United Kingdom

[3]*Alfred Wegener Institute, Helmholtz Centre for Polar and Marine Research, Bremerhaven, Germany

[4] Nansen Environmental and Remote Sensing Center and Bjerknes Center for Climate Research, Bergen, Norway

[5] UMR LOCEAN, Sorbonne Université, CNRS/IRD/MNHN, Paris, France

[6] National Research Council of Italy, Institute of Atmospheric Science and Climate (CNR-ISAC), Bologna, Italy

[7] Istituto Nazionale di Geofisica e Vulcanologia, Bologna, Italy

[8] Woods Hole Oceanographic Institution, Woods Hole, Massachusetts, U.S.A

[9] Department of Atmospheric Sciences, National Taiwan University, Taipei, Taiwan

[10] Department of Physics, National and Kaposdistrian University of Athens, Athens, Greece

[11] Ocean and Earth Science, National Oceanography Centre Southampton, University of Southampton, Southampton, United Kingdom

[12] National Oceanography Centre Southampton, University of Southampton, Southampton, United Kingdom

[13] Danish Meteorological Institute, Copenhagen, Denmark

[14] Nansen-Zhu International Research Center, Institute of Atmospheric Physics, Chinese Academy of Sciences, Beijing 100029, People's Republic of China

*Current affiliation
† Deceased, 23rd July 2021

This PDF file includes the following:

Table S1, Figs. S1 to S6, References (to)

**Table S1:** Details of the Eight Atmospheric models used for the analysis

| Model Name	CESM2-WACCM6	LMDZOR6	CAM6-Nor	EC-Earth3	CMCC-CM2-HR4	ECHAM6.3	HadGEM3	IAP4	Multi-model ensemble
Institution	WHOI-NCAR	LOCEAN-IPSL	NERSC	DMI	CMCC	MPI-M	UoS	NZC/IAP	--
Horizontal resolution (lat x lon)	0.95º x 1.25º (~100 km)	1.26º x 2.5º (~150 km)	0.94º x 1.25º (~100 km)	T255 (~80 km)	0.9° x 1.25° (~100 km)	T127 (~100km)	0.83º x 0.55º (~60 km)	~1.4 º x 1.4 º	Interpolated to 1.26º x 2.5º (~150 km)
# of vertical levels (top level)	70 (0.001 hPa)	79 (0.01 hPa)	32 (3.4 hPa)	91 (0.01 hPa)	30 (2 hPa)	95 (0.01hPa)	85 (85 km)	30 (2.2hPa)	--
# of ensemble members	30	30	20	20	10	10	10	15	145
Adjustment of SST/SIC	Yes	Yes	Yes	Yes	No	Yes	No	Yes	--
CMIP6 External Forcing used	CMIP6	HighRes MIP	CMIP6	CMIP6	HighRes MIP	CMIP6	HighRes MIP	1979-2005: CMIP5 historical 2006-2015: CMIP5 RCP8.5	--
Reference	Gettelman et al., 2019	Hourdin et al., 2020	Bentsen et al., 2013	Haarsma et al., 2020	Cherchi et al., 2019	Stevens et al., 2013 Müller et al., 2018	Walters et al., 2019	Sun, H. C., G. Q. Zhou, 2012	Liang et al., 2020
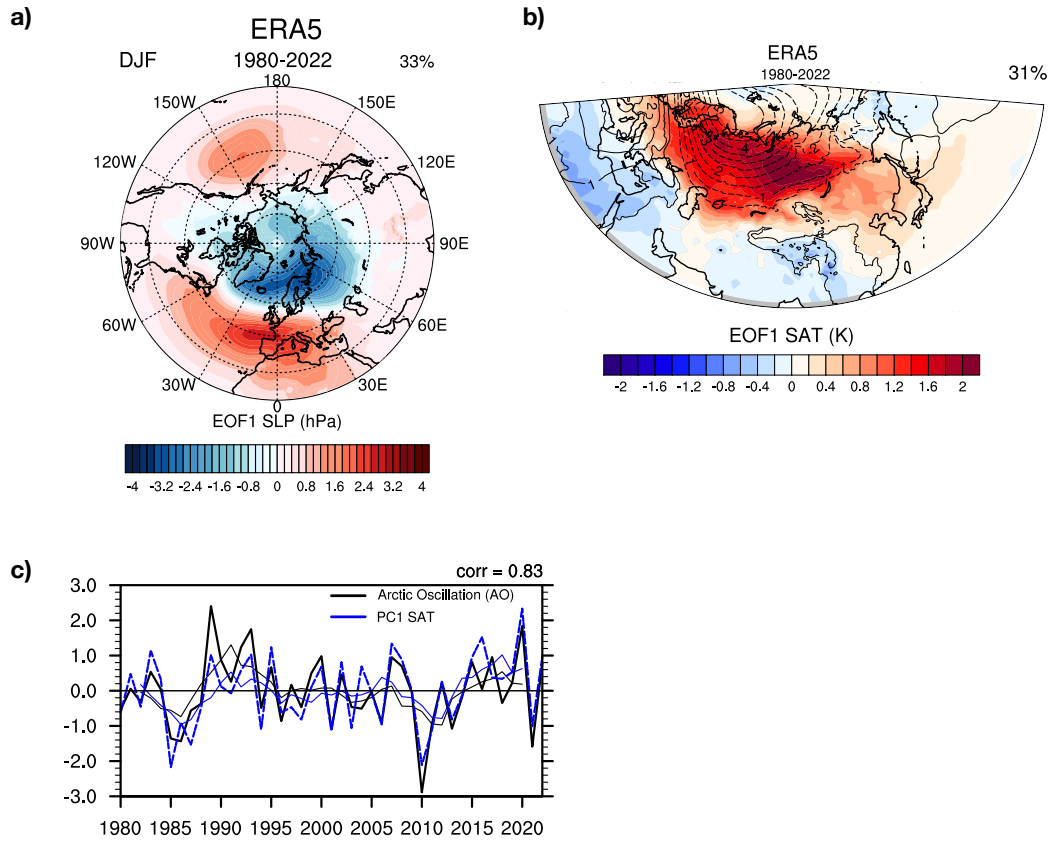
Fig S1 *In the ERA5 reanalysis for the period 1980 to 2022* **a)** *The EOF1 of observed winter (December-to-February) Northern Hemisphere (NH, 20˚N-90˚N, 180˚W-180˚E) SLP variability (known as Arctic Oscillation, AO) in hPa.* **b)** *the EOF1 of the observed winter Eurasian SAT variability in Kelvin (in shading) and contours show the associated sea level pressure anomaly, representing the AO. The top right of the figures mentions the explained variances.* **c)** *Associated time series of the PC1 NH SLP variability (in black) and the PC1 of the Eurasian SAT variability (in blue). The thin smoother time series represent the respective 5-year running means.*
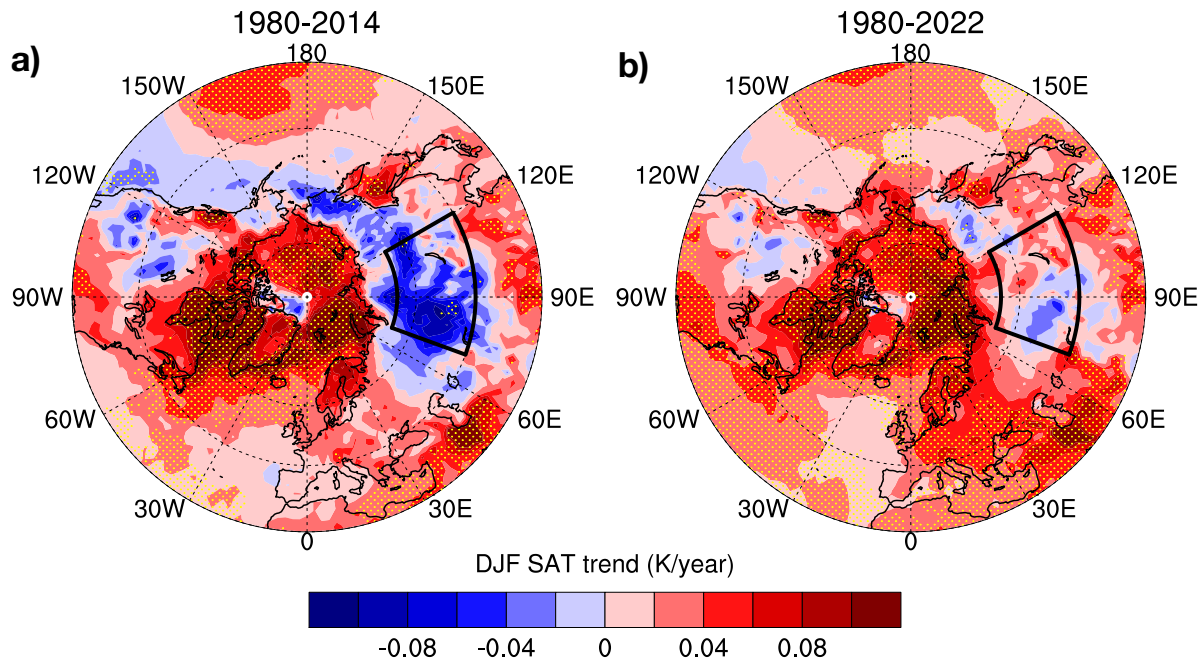
Fig S2 *a) In ERA5, DJF SAT trend for the period 1980 to 2014 (35 years) and b) 1980 to 2022 (43 years) in K/year. The trends in the yellow stippled regions are significant at a 5% level.*
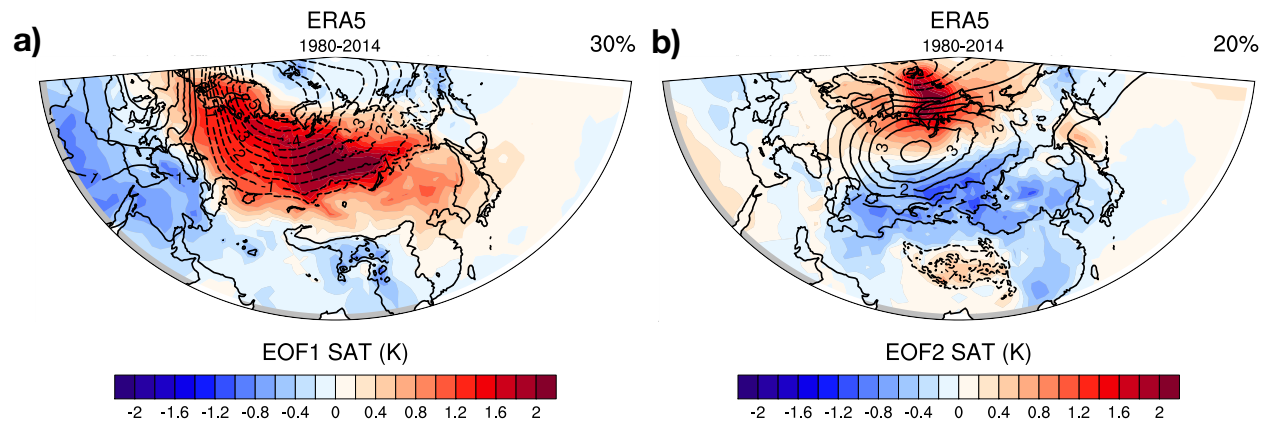

Fig S3 *The spatial patterns (in shading) of the a) EOF1 and b) EOF2/WACE of winter (DJF) SAT variability over Eurasia (20°-90°N, 0-180°E) in the ERA5 (1980-2014). The upper right corners of each panel show the explained variance. The EOF patterns are scaled to correspond to the one standard deviation variation of the respective PC time series and thus have units in K. The black contours are the SLP (in hPa) fields associated with the respective EOFs, derived by regression of the SLP field on the respective normalised PC time series.*

EOF2 SAT ALL
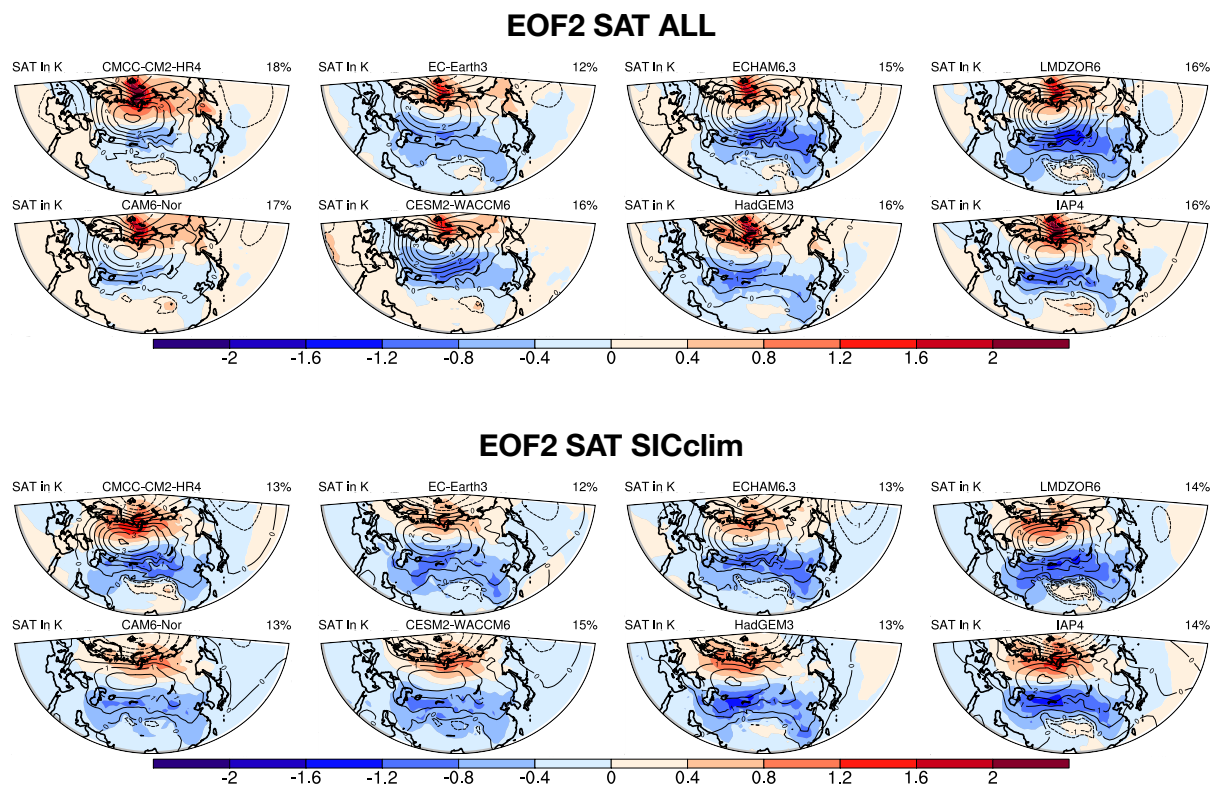
EOF2 SAT SICclim

Fig S4 *The EOF2 SAT/WACE pattern of variability (in shading) and its associated SLP pattern (in contours) in each model for **ALL** and **SICclim** experiments. The explained variance in each model are mentioned at the top right.*
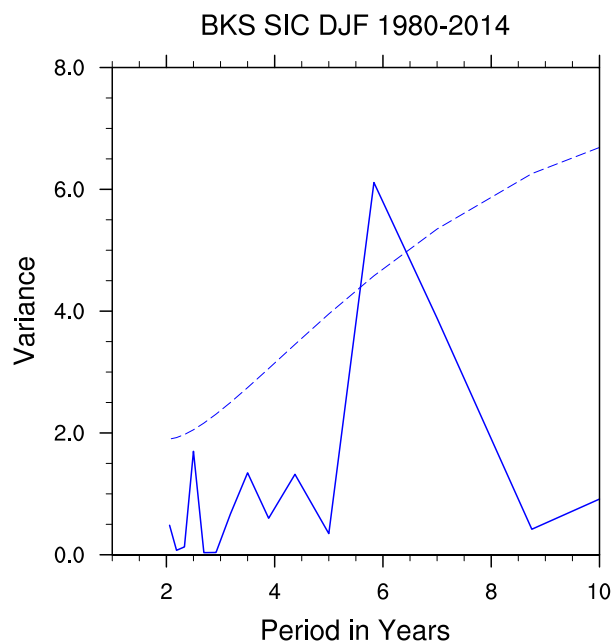
Fig S5 *Power spectrum of the winter BKS SIC anomaly (in blue) from HadISST1 from 1980 to 2014. The 95% confidence bound of the associated Markov spectrum is shown in a blue dashed line.*

5
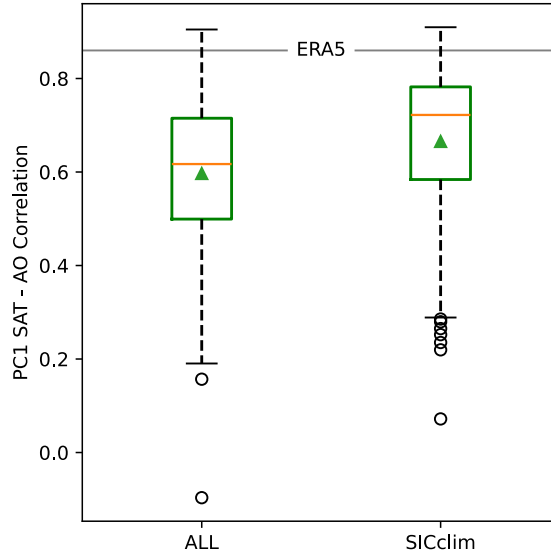
Fig S6 *Distribution of the correlation coefficient between Eurasian winter PC1 SAT and Arctic Oscillation (AO) in the multi-model large ensemble members for experiments ALL and SICclim. The multi-model ensemble median (orange line), interquartile range (green box) and full spread (whiskers) are shown through a box plot. The green triangles show the multi-model ensemble mean of the correlation. The horizontal black line indicates the same correlation in ERA5. The open circles show the outliers.*
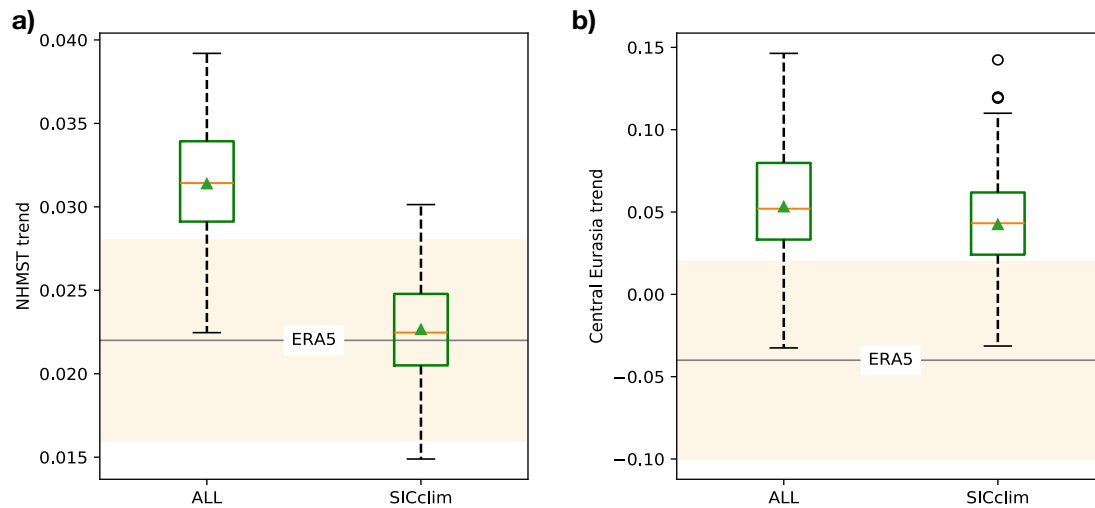
Fig S7*: The distribution of the **a)** Northern Hemisphere (0°-90°N, 0°-360°E) mean surface temperature (NHMST) trend and **b)** Central Eurasian (black box region in figure 2c,d, 45°N-65°N, 70°E-120°E) mean surface temperature trend in the multi-model large ensemble (145) members for **ALL** and **SICclim**. The multi-model ensemble median (orange line), interquartile range (green box) and full spread (whiskers) are shown through a box plot. The green triangles show the multi-model ensemble mean. The circles show the outliers. The horizontal black line indicates the same in ERA5 with its 95% confidence interval (light-shaded area). The units are in K/year.*

6

References:

Bentsen, M., Bethke, I., Debernard, J. B., Iversen, T., Kirkevåg, A., Seland, Ø., Drange, H., Roelandt, C., Seierstad, I. A., Hoose, C., & Kristjánsson, J. E. (2013). The Norwegian Earth System Model, NorESM1-M – Part 1: Description and basic evaluation of the physical climate. *Geoscientific Model Development*, *6*(3), 687–720. https://doi.org/10.5194/gmd-6-687-2013

Cherchi, A., Fogli, P. G., Lovato, T., Peano, D., Iovino, D., Gualdi, S., Masina, S., Scoccimarro, E., Materia, S., Bellucci, A., & Navarra, A. (2019). Global Mean Climate and Main Patterns of Variability in the CMCC-CM2 Coupled Model. *Journal of Advances in Modeling Earth Systems*, *11*(1), 185–209. https://doi.org/10.1029/2018MS001369

Gettelman, A., Mills, M. J., Kinnison, D. E., Garcia, R. R., Smith, A. K., Marsh, D. R., Tilmes, S., Vitt, F., Bardeen, C. G., McInerny, J., Liu, H. L., Solomon, S. C., Polvani, L. M., Emmons, L. K., Lamarque, J. F., Richter, J. H., Glanville, A. S., Bacmeister, J. T., Phillips, A. S., … Randel, W. J. (2019). The Whole Atmosphere Community Climate Model Version 6 (WACCM6). *Journal of Geophysical Research: Atmospheres*, *124*(23), 12380–12403. https://doi.org/10.1029/2019JD030943

Haarsma, R., Acosta, M., Bakhshi, R., Bretonnière, P. A., Caron, L. P., Castrillo, M., Corti, S., Davini, P., Exarchou, E., Fabiano, F., Fladrich, U., Franco, R. F., Garciá-Serrano, J., Von Hardenberg, J., Koenigk, T., Levine, X., Meccia, V. L., Van Noije, T., Van Den Oord, G., … Wyser, K. (2020). HighResMIP versions of EC-Earth: EC-Earth3P and EC-Earth3P-HR - Description, model computational performance and basic validation. *Geoscientific Model Development*, *13*(8), 3507–3527. https://doi.org/10.5194/GMD-13-3507-2020

Hourdin, F., Rio, C., Grandpeix, J.-Y., Madeleine, J.-B., Cheruy, F., Rochetin, N., Jam, A., Musat, I., Idelkadi, A., Fairhead, L., Foujols, M.-A., Mellul, L., Traore, A.-K., Dufresne, J.-L., Boucher, O., Lefebvre, M.-P., Millour, E., Vignon, E., Jouhaud, J., … Ghattas, J. (2020). LMDZ6A: the atmospheric component of the IPSL climate model with improved and better tuned physics. *Journal of Advances in Modeling Earth Systems*, e2019MS001892. https://doi.org/10.1029/2019ms001892

Liang, Y. C., Kwon, Y. O., Frankignoul, C., Danabasoglu, G., Yeager, S., Cherchi, A., Gao, Y., Gastineau, G., Ghosh, R., Matei, D., Mecking, J. V., Peano, D., Suo, L., & Tian, T. (2020). Quantification of the Arctic Sea Ice-Driven Atmospheric Circulation Variability in Coordinated Large Ensemble Simulations. *Geophysical Research Letters*, *47*(1), 1–10. https://doi.org/10.1029/2019GL085397

Müller, W. A., Jungclaus, J. H., Mauritsen, T., Baehr, J., Bittner, M., Budich, R., Bunzel, F., Esch, M., Ghosh, R., Haak, H., Ilyina, T., Kleine, T., Kornblueh, L., Li, H., Modali, K., Notz, D., Pohlmann, H., Roeckner, E., Stemmler, I., … Marotzke, J. (2018). A Higher-resolution Version of the Max Planck Institute Earth System Model (MPI-ESM1.2-HR). *Journal of Advances in Modeling Earth Systems*, *10*(7), 1383–1413. https://doi.org/10.1029/2017MS001217

Stevens, B., Giorgetta, M., Esch, M., Mauritsen, T., Crueger, T., Rast, S., Salzmann, M., Schmidt, H., Bader, J., Block, K., Brokopf, R., Fast, I., Kinne, S., Kornblueh, L., Lohmann, U., Pincus, R., Reichler, T., & Roeckner, E. (2013). Atmospheric component of the MPI-M earth system model: ECHAM6. *Journal of Advances in Modeling Earth Systems*, *5*(2), 146–172. https://doi.org/10.1002/jame.20015

Sun, H. C., G. Q. Zhou, and Q. C. Z. (2012). Assessments of the climate system model (CAS-ESM-C) using IAP AGCM4 as its atmospheric component. *Chin. J. Atmos. Sci*, *36*, 215–233.

Walters, D., Baran, A. J., Boutle, I., Brooks, M., Earnshaw, P., Edwards, J., Furtado, K., Hill, P., Lock, A., Manners, J., Morcrette, C., Mulcahy, J., Sanchez, C., Smith, C., Stratton, R., Tennant, W., Tomassini, L., Van Weverberg, K., Vosper, S., … Zerroukat, M. (2019). The Met Office Unified Model Global Atmosphere 7.0/7.1 and JULES Global Land 7.0 configurations. *Geoscientific Model Development*, *12*(5), 1909–1963. https://doi.org/10.5194/gmd-12-1909-2019